# The static preload associated myogenic spontaneous fasciculation response in lengthening cardiac muscle

**Shouyan Fan**
Hainan Medical University
**Lingfeng Gao**
Hainan Medical University
**Annie Christel Bell**
Hainan Medical University
**Joseph Akparibila Azure**
Hainan Medical University
**Yang Wang** ( katotds@sina.com )
Hainan Medical University

**Research Article**

**Keywords:** cardiac papillary muscle, mechanical stepping stretch, myogenic spontaneous force

**Posted Date:** March 3rd, 2021

**DOI:** https://doi.org/10.21203/rs.3.rs-257074/v1



**Version of Record:** A version of this preprint was published at Scientific Reports on July 20th, 2021. See the published version at https://doi.org/10.1038/s41598-021-94335-w.

# Abstract

The passive tension force enhancement is one kind of myogenic spontaneous fasciculation in muscles. However, its physiological properties in cardiac fibres are not well known. In this study, mice cardiac papillary muscle spontaneous force enhancement was evaluated by micro stepping stretch method. The occurrence of spontaneous force and real time cardiac fibre $Ca^{2+}$ redistribution was tranced by Flou-3 (2mM) indicator. Force enhancement amplitude, enhancement prolonging time, and tension–time integral were analysis by myograph analyser. The results indicated that the spontaneous force occurred immediately after the active stretch, rapidly enhanced during tolerating the sustained static stretch. The force occurrence and amplitude enhance synchronized with the $Ca^{2+}$ recruitment and lightning transmitted to adjacent fibres. In high preload fibres, the enhancement was forceful to over its maximum passive tension (6.20 ± 0.51 $N/mm^2$ to 4.49 ± 0.43 $N/mm^2$). The force occurrences were unsteadiness in each stretch. The increased enhancement amplitude combining with the shortening prolonging time induced reduction of tension–time integral. We concluded that the intracellular $Ca^{2+}$ synchronized force enhancement is one kind of interruption event in overloading cardiac fibres. This interruption occurred during the relaxation processing in cardiac muscle, therefore affect the rhythmic stability of cardiac relaxation-contraction cycle.


# Introduction

The isolated muscle fibre has the mechanical properties to generate enhanced myogenic spontaneous tension under the lengthening stretch. When instantaneous stretch the muscle fibre beyond of its optimum length, a significant myogenic twitch can be observed [1]. This spontaneous twitch concept is widely mentioned in isolated striated muscle fibre [2], muscle-tendon unit [3], flexor muscles [4, 5] and in skinned muscle fibres as well [6]. It is considered that the spontaneous twitch is the mechanical response of sarcomere rearrangement and elastic properties in the muscle bundles [7]. Mechanical stretched muscle fibre induce differences of sarcomere length in elongation, increased recruitment of myosin heads occurred [8, 9]. In the lengthened muscle fibres, passive tension sustained its intensity because the concentrated $Ca^{2+}$ bonding altered calcium sensitivity in sarcomeric myofilaments [10, 11], and the $Ca^{2+}$ binding to myosin-actin sites is not attenuated [12]. However, the myogenic spontaneous force enhancement occurrence was rarely verified in cardiac muscles.

In the conventional view of cardiac diastole, muscle relaxation was regarded as a mere passively and an essential step in the cardiac cycle. The intracellular calcium decline, thin filament deactivation, and cross-bridge cycling kinetics are actively regulated [13], therefore created conditions for force enhancement emergence in the muscle fibres. When in the late diastole, cardiac ventricular wall tolerates transient excessive mechanical load which was mentioned as “kick from atrium” [14]. In Fig. 1A the excessive load within ventricle is from a transient increasing of atrium (the dot curve from ϕ to ▯, * was the maximum of transient atrial pressure; arrow mark is atrial equivalent point of “kick from atrium” to ventricular diastole pressure). Figure 1B is the muscle velocity of one cycle in cardiac ventricle. The “kick from atrium” decelerated ventricle relaxation (Fig. 1B, curve between **a** and **b** presented the deceleration). In diastolic

muscle, the strengthened “kick” bring out the condition to occurring the spontaneous force enhancement. In heart failure people who were with normal ejection fraction, fitness exercise induced an abnormal increasing of end diastolic pressure. This specific end diastolic pressure increasing pertain to the decompensating of cardiac muscle relaxation [15]. The myogenic spontaneous force occurrence perhaps prefigures the cardiac muscle fatigue in the early stage of decompensating.

In this study, we investigated the spontaneous force occurrence in lengthening tolerated cardiac fibres. We hypothesis that the occurrence is a myogenic spontaneous process in static preload cardiac muscle. Its enhancement is significant relative to the static preload.

# Results

### 1. The spontaneous force occurrence in low preload range

1.1 As show in Fig. 3A, under the low preload, active stretch engenders a passive tension peak (**I** active stretch on time scale, * passive tension amplitude peak). A subsequently passive tension attenuated after the peak (**II**, passive tension attenuation on time scale). A myogenic spontaneous force occurred during passive tension attenuated (FE in Fig. 3A). The 1st stretched $\mathbf{PT_{max}}$ was 1.19 ± 0.14 N/mm$^2$, force enhancement amplitude $\mathbf{A_{IFE}}$ 1.11 ± 0.16 N/mm$^2$, enhancement prolonged 123.72 ± 4.58 msec, total attenuation (II) was 216.51 ± 9.44 msec, therefore **t** possessed 57.14% of relaxation on time scale. 1st, 2nd and 3rd force enhancement tension-time integral **TTI** was 22.01 ± 0.73 N/mm$^2$·sec, 24.04 ± 1.21 N/mm$^2$·sec and 26.88 ± 1.48 N/mm$^2$·sec respectively.

1.2 In shed muscle fibres, although the fibre tolerated almost same preload as in intact fibres, and $\mathbf{PT_{max}}$ presented a perfect linear correlation throughout the preload range (Fig. 4C, $R^2$ = 0.99; hollow square, $\mathbf{PT_{max}}$), force enhancement significantly declined. The shed fibres $\mathbf{A_{IFE}}$ were lower than occurrences in intact fibres (Fig. 4C, black square), **TTI** was reduced as well (Fig. 5A, solid square in low preload; 19.22 ± 0.72 N/mm$^2$·sec, 20.20 ± 0.61 N/mm$^2$·sec and 22.36 ± 1.27 N/mm$^2$·sec in 1st, 2nd and 3rd stretch respectively). Force enhancement prolonging time **t** were extended on time scale.

The stretched force enhancement waveform values were summarized in Table 1.

Table 1

| Preloading condition | Preparation | Stretch | $PT_{max}$ ( $N/mm^2$) | $A_{IFE}$ ( $N/mm^2$) | FE prolonged time | |
|---|---|---|---|---|---|---|
| | | | | | t (msec) | % of II |
| Low preload range | Intact muscle | 1st | 1.19 ± 0.14 | 1.11 ± 0.16 | 123.72 ± 4.58 | 57.14 |
| | | 2nd | 1.40 ± 0.19 | 1.21 ± 0.17 | 132.51 ± 4.51 | 69.23 |
| | | 3rd | 1.51 ± 0.21 | 1.31 ± 0.37 | 141.20 ± 5.33 | 83.33 |
| | Shed muscle | 1st | 1.25 ± 0.35 | 0.48 ± 0.03 | 126.88 ± 6.79 | 72.73 |
| | | 2nd | 1.47 ± 0.46 | 0.50 ± 0.04 | 130.89 ± 5.41 | 53.94 |
| | | 3rd | 1.58 ± 0.50 | 0.58 ± 0.09 | 138.17 ± 7.61 | 44.44 |

### 2. The $[Ca^{2+}]_i$ redistribution in sustained static stretch muscle bundle

Figure 3B is the fluorescence image of $[Ca^{2+}]_i$ before active stretch. $[Ca^{2+}]_i$ have no significant changes during the static preload, however the recruitment and redistribution immediately occurred after active stretch (Fig. 3C, the space between * marks was the $[Ca^{2+}]_i$ fluorescence image vision area). After the active stretch, $[Ca^{2+}]_i$ assembled in the cardiac fibres, rapidly transmitted to the adjacent cardiac cells during the fibre tolerating static stretch. The $[Ca^{2+}]_i$ sparkling transmitted in the fibre longitudinally (Fig. 3D, dot marked $[Ca^{2+}]_i$ sparkling area; arrow means transmit dimension) to the adjacent myocytes.

### 3. The spontaneous force in high preload range

Figure 4A is the typical force enhancement waveform in high preload cardiac fibre. The $\mathbf{PT_{max}}$ presented a perfect linear correlation throughout preload range (Fig. 4B, $\mathbf{PT_{max}}$, black hollow circle, $R^2 = 0.99$), however $\mathbf{A_{FE}}$ did not indicated the linear relationship (solid dots).

3.1 In intact fibre, force enhancement was unstable. In the most strengthened stretch, force enhancement surpassed its passive tension, therefore significantly disrupted the amplitude in relaxation process (2nd $\mathbf{PT_{max}}$ and $\mathbf{A_{FE}}$ was 4.49 ± 0.43 $N/mm^2$, 6.20 ± 0.51 $N/mm^2$ respectively). The 1st and 2nd force enhancement **TTI** was not significantly increased in high preload fibres (27.45 ± 0.84 $N/mm^2$·sec, 25.90 ± 0.95 $N/mm^2$·sec respectively). 2nd **TTI** reduced 5.65% (Fig. 5A, solid dots tagged with 1st and 2nd, *** means $p < 0.001$). Force enhancement prolonging time (**t**) were reduced than its in low preload range. However, the $\mathbf{t_2}$ shortened 7.60% than $\mathbf{t_1}$ (Fig. 5B, solid dots tagged with 1st and 2nd ). In high preload fibre, the difference of force enhancement prolonging time was significantly enlarged, which indicated the instability of the passive tension in cardiac muscle fibres

3.2 In shed cardiac fibres, although it tolerated same preload as in intact muscle fibres, $\mathbf{PT_{max}}$ presented a perfect linear correlation throughout the preload range (Fig. 4C, $R^2 = 0.99$; hollow square, $\mathbf{PT_{max}}$), force enhancement significantly declined as well. 1st $\mathbf{A_{FE}}$ either 2nd $\mathbf{A_{FE}}$ did not over its $\mathbf{PT_{max}}$ (2.42 ± 0.19 $N/mm^2$ and 3.89 ± 0.31 $N/mm^2$ in 1st stretch, 2.55 ± 0.31 $N/mm^2$ and 4.11 ± 0.22 $N/mm^2$ in 2nd stretch respectively).

The force enhancement **TTI** was 28.43 ± 0.49 $N/mm^2$·sec and 26.26 ± 0.78 $N/mm^2$·sec in 1st and 2nd stretch respectively (Fig. 5A, solid square in high preload). 2nd **TTI** reduced 7.63%. Force enhancement prolonging time **t** were extended in each stretch, however because the II was significantly extended either, **t** shared % of II were reduced. The details are summarized in Table 2.

Table 2

| Preloading condition | Preparation | Stretch | $PT_{max}$ ( $N/mm^2$) | $A_{IFE}$ ( $N/mm^2$) | FE prolonged time | |
|---|---|---|---|---|---|---|
| | | | | | t (msec) | % of II |
| High preload range | Intact muscle | 1st | 4.40 ± 0.60 | 3.03 ± 0.48 | 127.08 ± 8.31 | 65.82 |
| | | 2nd | 4.49 ± 0.43 | 6.20 ± 0.51*** | 117.42 ± 10.80 | 21.89 |
| | Shed muscle | 1st | 3.89 ± 0.31 | 2.42 ± 0.19 | 105.29 ± 11.10 | 15.52 |
| | | 2nd | 4.11 ± 0.22 | 2.55 ± 0.31 | 99.20 ± 9.90 | 10.14 |

## 4.The briefing of CfTX-1 peptide

The *CfTX-1* peptide sequence was first identified from the Hainan island local *Aurelia aurita* tentacles (*A. aurita*, captured in the northern coast of Hainan Province, China).

In brief, frozen *A. aurita* tentacles were placed in an autolysis solution + 4℃ overnight. After centrifuged at 20,000×g for 1 h at 4°C. The derived resultant supernatant was immediately frozen at − 80°C in a condenser chamber and vacuum to extreme dryness (VirTis Bench Top freeze dryer, SP industries, Inc., PA, U.S.A..). The lyophilized crude venom was 10% polyacrylamide gel analysed. The *CfTX-1* peptide sequence was identified from the 43 kDa band. It was a 11 amino acids polypeptide that had a high overlap with the positive strain of amino acid sequences 304–314 (*IFNFFDLmKVK*) of *CfTX-1* (UniProtKB-A7L035). This *CfTX-1* 11 amino acids were further synthesized by a commercial resin solid-phase method, then finally lyophilized and quality control analysed by HPLC and Electrospray Ionization Tandem Mass Spectrometry (ESI-MS).

The synthesized *CfTX-1 peptide* indicated a strong effect on cell membrane to induced a hyperpolarization in urothelial membrane *in vitro*[16], and improve the mice cardiac diastole *in vivo* as well.

# Discussion

In 1950s, Abbott et al. first mentioned an excess of tension generation appreciably greater than the tension developed in 1.9 mm/sec stretched toad sartorius [17]. Hill et al. reported an enhanced energy liberated and a transient increasing of tension when the toad sartorii obtain a 5 mm lengthening stretch within 393 msec [18]. Decades later, Sugi's experiment testified semitendinosus fibre tension rising to the initial isometric value after a fell below the initial isometric level at the end of an 80–150 cm/sec stretch (0.8–1.5 mm/msec) and a delayed transient tension rising in a 30–60 cm/sec (0.3–0.6 mm/msec) stretch [19], therefore, fundamentally validated the mechanical lengthening velocity relation with the occurrence of force enhancement. In this study we use a program controlled micro stepping motor to obtain a stable mechanical lengthening velocity for each active stretch. The velocity 5μm/msec is the valid condition for testing the spontaneous force occurrence in intact and shed cardiac muscle fibres. A similar experimental method was ponderingly used in Edman's experiments, who was aware of the residual force enhancement from the non-uniform distribution of the myofilament during the length change [20]. Recent researches gradually revealed the force enhancement corresponding to the magnitude of the stretch [21]. This correspondent is because of muscle fibre half-sarcomere non-uniformities, and the sarcomeric component associated $Ca^{2+}$-induced stiffness [22]. In addition, force enhancement did not increase with stretch amplitude on the ascending limb, but on the descending limb of the force–length relationship [23]. One conclusion emerges from above summarized results that force enhancement occurrence is more significant in increased preload muscle fibres, and this enhancement originated from the deficient myofibril cross-bridge interaction. Our study proved the existence of the enhancement in increased preload cardiac muscle fibres, furthermore we found the instability of the force enhancement in high preloading cardiac muscle. This discrepancy of force enhancement interrupted the cardiac muscle during its relaxation process. The interruptions are mainly manifested in several aspects: 1) The enhanced force amplitude disrupted the unconstipated passive tension waveform in cardiac muscle; 2) Affect the passive tension attenuation time (The II in Fig. 3); 3) Scrambled the rhythmicity of $Ca^{2+}$ signalling in lengthened cardiac myocytes.

**TTI** is the index for evaluating the time dependence of the muscle tension. This index was used for determining the muscle energy output in its isometric contractions [24], to determine the capacity ratio of the diaphragm [25], analysing the transient contraction [26], and evaluating the effects of contractile filament mutations on muscle twitch [27]. In cardiac muscle, **TTI** determinate the onset of contractions in diastole-systolic cycle [28, 29]. Our results suggest that this index significant depend on excessive lengthening load. It was in a precarious state in high preload cardiac fibres. **TTI** variation reflects the calcium sensitivity interruption during tension development [30], is the index of fatigue development [31]. The increasing of TTI in high preload stretched fibres demonstrated an $Ca^{2+}$ signalling involved extra energy consumption during tolerating lengthening.

In addition, *CfTX* have the homology structure that is with three-domain Cry toxins (δ-endotoxins) and α-helices in N-terminal domain [33, 34]. This type of pore-forming toxin was reported accelerated the first temporal derivative of the isosmetric contraction (dP/dt) [32]. Its specific lipid-dependent cell penetration induces a transient membrane leakage for cardiomyocyte interaction at the atomic level, involved in isometric force [35], contributed to intracellular $Ca^{2+}$ release, improving cAMP and PKA activity in cardiomyocytes [36]. The shed cardiac muscle fibre tolerating tests shown this compound reduced the force enhancement and its relative index in high preload condition. The *CfTX* compound may play an important role in improving cardiac muscle passive tension stability.

# Methods

### 1. Mice cardiac papillary muscle bundle preparation

The animal experiment was reviewed and approved by the Hainan medical university institutional ethics board.
Animal care was according with the ethical principles of the guide for the care and use of laboratory animals (8th Edition, International Standard Book Number-13: 978-0-309-15401-7$4.
All procedures performed were conformed to the guidelines from directive 2010/63/EU of the European Parliament on the protection of animals used for scientific purposes.
The animal study was conducted according to ARRIVE guidelines.
After the mice anaesthesia by 3% Pentobarbital sodium, intraperitoneal injection (0.1ml/15g body weight). The corneal reflex disappears was for monitoring aesthetic depth. The physical method of cervical dislocation was used for mice euthanasia.

The cardiac papillary muscles strips were isolated from the *Kunming* mice left ventricle (n = 10, male, 4 weeks, SPF grade), then prepared to 0.5mm diameter intact fibres. For shed preparation, fibres were suspension in synthesized 35 mmol *CfTX-1* peptide solution (peptide sequence *IFNFFDLmKVK*), 4°C 5 min. All fibres were finally stabled in *Ringer's* solution before the tolerance tests.

The tolerance test was operated on a stepper motor driving roller screw platform. Cardiac fibre one end fixed to the glass probe which was fastened to a roller screw module; the other end hooked on the reed of Wheatstone bridge-type piezoelectric strain sensor (Model number JH-2 10g, Beijing aerospace medical engineering institute, Beijing China). The fibres were kept horizontally on a 4°C chilled glass slide.

The series mechanical stretch is operated by stepper motor which was controlled by Arduino Uno R3 board (Arduino, Allchips Ltd., Hong Kong).
In order to obtain the steady mechanical lengthening in each active stretch, the strengthen of the stretch was determined by the rotating speed and the angles of stepper motor shaft which was driven by programmed pulse frequency of the Arduino board.
Cardiac fibres tolerated 0.05mm, 5μm/msec linear lengthening in each active stretch.

### 2. Muscle mechanical stretch and the myograph analysis

As the schematic diagram of mechanical stretch shown in Fig. 2, slack cardiac fibres were slowly lengthened to remain taut, and obtained 1 gram(g) preload (Fig. 2, ▯ on Y axis). The fibre length under this 1g is defined as initial length ($L_0$). The initial length fibres were stabled on a slide glass, and suspended in *Ringer*'s solution before tests.

The fibres were slowly lengthening 20% of its $L_0$ with micro tuner, to obtained a static preload (Fig. 2, ▯ on Y-axis). This length defined as low preload ($L_l$). The low preload fibres obtained an rapid transient lengthening (0.05mm lengthening with the velocity of 5μm/msec), which is defined as active stretch (Fig. 2,solid lined arrow). Fibres subsequently tolerated the static lengthening, which is defined as sustained static stretch (Fig. 2, dot lined arrow). The active stretch repeated three times. After that, fibres further lengthened 40% to obtain a higher static preload ($L_h$). The high preload fibres obtained active stretch. The stretch repeated twice. The fibres passive tension trajectories (myograph) were recorded by a polygraph device (BL-420s, data acquisition & analysis system, Chengdu TME technology Co. Ltd., Chengdu, China).

The passive tension maximum amplitude ($\mathbf{PT_{max}}$), myogenic spontaneous force enhancement amplitude ($\mathbf{A_{FE}}$), prolonging time (**t**), myogenic spontaneous force tension–time integral (**TTI**) were processed and calculated by TM_WAVE software (Chengdu techman software Co., Ltd., Chengdu China).

### 3. Real-time visualization of $[Ca^{2+}]_i$ recruitment

Mechanical stretch induced cardiac fibre $Ca^{2+}$ ($[Ca^{2+}]_i$) recruitment was real time visualized by fluorescence excitation. Before the stretching tests, fibres were suspended on the support glass slide, bath in 2mM Flou-3 AM/DMSO solution 20min. The fibres excited by 499nm LED light beam to obtain a 528nm emission wavelength luminescence. The fluorescence imaging of spatial dynamics of $[Ca^{2+}]_i$ in stretching fibres were captured by an inversion microscope system (XDS-1B, Chongqing Coic industrial Co., Ltd. Chongqing China), photographed by a 1200 TVL resolution camera connected high-speed analogue video system (SV2000E video capture system, Tairong Technology, Xuzhou, Jiangsu China). The light beam excited fluorescence bright area exhibited the activation of $[Ca^{2+}]_i$ in stretching fibres. For reducing the phototoxicity and dye bleaching to a minimum, the fibres were illuminated at low power. The activated $[Ca^{2+}]_i$ redistribution imaging was captured simultaneously with the myograph. Because the obtained fluorescence brightness was high speed images in the suspended cardiac fibres, the absolute $[Ca^{2+}]_i$ concentrations could not be quantified by this method. However, the real time $[Ca^{2+}]_i$ qualitative analysis can be done in stretching fibres. The fluorescence images were processed via ImageJ (Ver. 1.53a, Wayne Rasband, NIH, U.S.A.).

### 4. Statistical analysis

The values present as mean ± SEM. The value differences under the preload conditions are analysed by using unpaired *t*-test method (Excel 2013, 2012 Microsoft Corporation). $p < 0.001$ indicated a significant difference.

# Declarations

**Acknowledgement:**

This work was supported by Hainan province key R&D project (ZDYF2017121).

**Authors' contributions**

Shouyan Fan carried out the study design, data collection and analysis, isolated cardiac muscle fibre preparations, participated in the draft of the manuscript.

Lingfeng Gao, Annie Christel Bell, and Joseph Akparibila Azure prepared the mice cardiac papillary muscle fibres and designed the stretching analysis, operated the lengthening tests.

Yang Wang, leader of the research team, organizing the references studies, the participated in the design of the experiment model, statistical analysis and involved in draft of manuscript.

All authors read and approved the final manuscript.

**Conflicts:**

The authors do not have any conflicts of interest.

**Data availability statement**

The data that support the findings of this study are openly available in figshare at http://doi.org/10.6084/m9.figshare.14058197

# References

1. Edman, K.A., & Flitney, F.W. Non-uniform behaviour of sarcomeres during isometric relaxation of skeletal muscle. *J. Physiol.* **276**, 78-79 (1978).
2. Noble, M.I. Enhancement of mechanical performance of striated muscle by stretch during contraction. *Exp. Physiol.* **77(4)**, 539-552 (1992).
3. Mahmood, S., Sawatsky, A., & Herzog, W. Increased force following muscle stretching and simultaneous fibre shortening: Residual force enhancement or force depression – That is the question? *J. Biomech.* **116**, 110216 (2021).
4. Fortuna, R., Powe,r G.A., Mende, E., Seiberl, W., & Herzog, W. Residual force enhancement following shortening is speed-dependent. *Sci. Rep.* **12**, 21513 (2016).
5. Hahn. D., & Riede,l T.N. Residual force enhancement contributes to increased performance during stretch-shortening cycles of human plantar flexor muscles in vivo. *J. Biomech.* **22(77)**, 190-193 (2018).
6. Fukutani, A., Joumaa, V., & Herzog, W. Influence of residual force enhancement and elongation of attached cross-bridges on stretch-shortening cycle in skinned muscle fibers. 2017 https://doi.org/10.14814/phy2.13477.

7. Kulke, M. *et al*. Interaction between PEVK-titin and actin filaments: origin of a viscous force component in cardiac myofibrils. Circ Res 2001; 89(10), 874-881.
8. Brown, L.M., & Hill, L. Some observations on variations in filament overlap in tetanized muscle fibres and fibres stretched during a tetanus, detected in the electron microscope after rapid fixation. J Muscle Res Cell Motil 1991; 12(2):171-182.
9. Campbell, K.S., Janssen, P.M.L., & Campbell, S.G. Force-dependent recruitment from the myosin off state contributes to length-dependent activation. Biophys J 2018;115(3), 543-553.
10. Edman, K.A.P., & Caputo, C. Release of calcium into the myofibrillar space in response to active shortening of striated muscle. Acta Physiol 2017; 221(2), 142-148.
11. Stienen, G.J. Pathomechanisms in heart failure: the contractile connection. J Muscle Res Cell Motil 2015; 36(1), 47-60.
12. Edman, K.A.P., & Caputo, C. Release of calcium into the myofibrillar space in response to active shortening of striated muscle. Acta Physiol 2017; 221(2), 142-148.
13. Biesiadecki, B.J., Davis, J.P., Ziolo, M.T., & Janssen, P.M.L. Tri-modal regulation of cardiac muscle relaxation; intracellular calcium decline, thin filament deactivation, and cross-bridge cycling kinetics. *Biophys. Rev.* **6**, 273-289 (2014).
14. Leite-Moreira, A.F. Current perspectives in diastolic dysfunction and diastolic heart failure. Heart 2006; **92,** 712-718.
15. Westermann, D. *et al*. Role of left ventricular stiffness in heart failure with normal ejection fraction. *Circulation*. **117**, 2051-2060 (2008).
16. Shen, Z.D. *et al*. The urothelium enhancive polarization in CfTX-1 peptide intervened toad urinary bladder. *Afr. J. Biotechnol.* **18**, 695-701 (2019).
17. Abbott, B.C., & Aubert, X.M. The force exerted by active striated muscle during and after change of length. *J. Physiol.* **117**, 77–86 (1952).
18. Hill, A.V., & Howarth, J.V. The reversal of chemical reactions in contracting muscle during an applied stretch. *Proc. R. Soc. Lond. B.* **151**, 169–193 (1959).
19. Sugi, H. Tension changes during and after stretch in frog muscle fibres. *J. Physiol.* **225**, 237–253 (1972).
20. Edman, K.A.P., & Tsuchiya, T. Strain of passive elements during force enhancement by stretch in frog muscle fibres. *J. Physiol.* 490, 191–205 (1996).
21. Herzog, W., & Leonard, T.R. Force enhancement following stretching of skeletal muscle: a new mechanism. *J. Exp. Biol.* **205**, 1275-1283 (2002).
22. Herzog, W., Lee, E.J., & Rassier, D.E. Residual force enhancement in skeletal muscle. J. Physiol. 574, 635-642 (2006).
23. Hisey, B., Leonard, T.R., & Herzog, W. Does residual force enhancement increase with increasing stretch magnitudes? *J. Biomech.* **42**, 1488-1492 (2009).
24. 24. Gibbs, C.L., & Gibson, W.R. Effect of alterations in the stimulus rate upon energy output, tension development and tension-time integral of cardiac muscle in rabbits. *Res.* **27**, 611-618 (1970).

25. Harikumar, G. *et al*. Tension-time index as a predictor of extubation outcome in ventilated children. *Am. J. Respir. Crit. Care Med*. **180**, 982-988 (2009).
26. Horiuti, K. Some properties of the contractile system and sarcoplasmic reticulum of skinned slow fibres from Xenopus muscle. *J. Physiol.* **373**, 1–23 (1986).
27. Sewanan, L.R., Moore, J.R., Lehman, W., & Campbell, S.G. Predicting Effects of Tropomyosin Mutations on Cardiac Muscle Contraction through Myofilament Modeling. *Front Physiol.* **7**, 473 (2016).
28. 28. Suga, H. *et al*. Force-time integral decreases with ejection despite constant oxygen consumption and pressure-volume area in dog left ventricle. *Res.* **60**, 797-803 (1987).
29. Alpert, N.R., Blanchard, E.M., & Mulieri, L.A. Tension-independent heat in rabbit papillary muscle. *J. Physiol*. **414**, 433-453 (1989).
30. Powers, J.D. *et al*. Modulating the tension-time integral of the cardiac twitch prevents dilated cardiomyopathy in murine hearts. *J.C.I. Insight.* **5**: e142446 (2020).
31. Hepple, R.T. *et al*. The $O_2$ cost of the tension-time integral in isolated single myocytes during fatigue. *Am. J. Physiol. Regul. Integr .Comp. Physiol*. **298**, R983-988 (2010).
32. Gomes, H.L. *et al*. Cardiovascular effects of Sp-CTx, a cytolysin from the scorpionfish (Scorpaenaplumieri) venom. *Toxicon.* **118**, 141-148 (2016).
33. Brinkman, D.L. *et al*. Chironex fleckeri (box jellyfish) venom proteins: expansion of a cnidarian toxin family that elicits variable cytolytic and cardiovascular effects. *J. Biol. Chem.* **289**, 4798-4812 (2014).
34. Andreosso, A. *et al*. Structural Characterisation of Predicted Helical Regions in the Chironex fleckeri *CfTX-1* Toxin. *Mar. Drugs.* **16**, 201 (2018).
35. Wu, P.L., Chiu, C.R., Huang, W.N., & Wu, W.G. The role of sulfatide lipid domains in the membrane pore-forming activity of cobra cardiotoxin. *Biochim. Biophys. Acta*. **1818**, 1378-13850 (2012).
36. Wang, Q., Zhang, H., Wang, B., Wang, C., Xiao, L., & Zhang, L. β adrenergic receptor/cAMP/PKA signaling contributes to the intracellular $Ca^{2+}$ release by tentacle extract from the jellyfish Cyanea capillata. *BMC Pharmacol. Toxicol.* **18**, 60 (2017).

# Figures

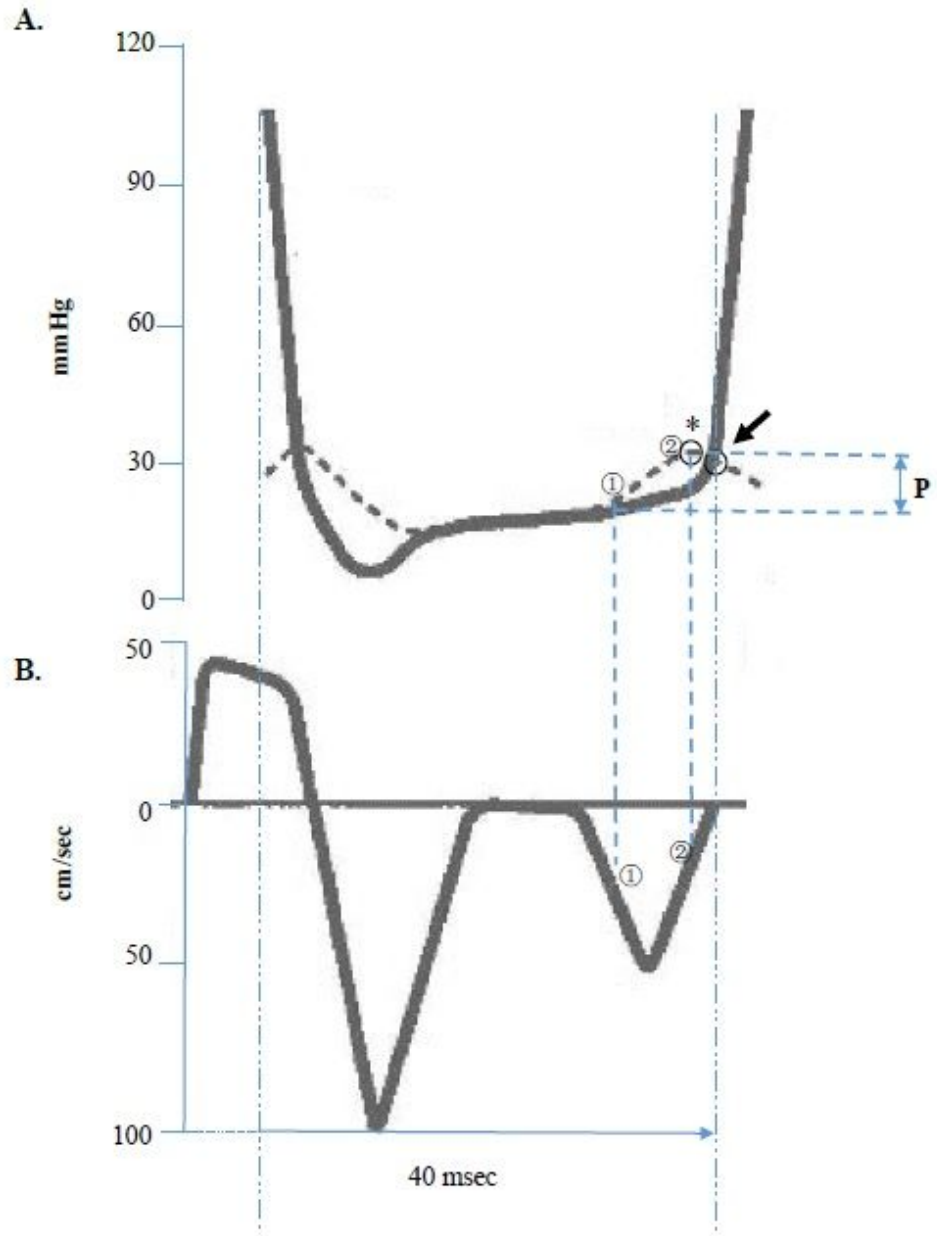


## Figure 1

Illustration of the excessive load in late diastole and relative muscle relaxation velocity in cardiac ventricle A. Left ventricle pressure (solid curve) and left atrial pressure (dotted curve) in ventricular diastolic phase. The marked ① and ② represent the rising atrial systolic pressure (kick from atrium), * was the maximum of atrial systolic pressure. ① was the equilibrium point of atrial pressure to the moment ventricular pressure. The ventricle was significantly contracted after the equilibrium point ①. Symbol P indicated the kick amplitude (excessive load amplitude) in ventricle late diastole phase. B. The ventricle muscle relaxation velocity in each diastole and systole cycle. a and b was the relaxation velocity response to ① and ②. The ventricular muscle velocity was significantly reduced because of excessive load from the kick (comparing with a' and b' in primary diastolic phase). The duration between a and b indicated the kick time (excessive

load time) in ventricle late diastole phase. The images originated from Leite-Moreira AF [14] and was modified.

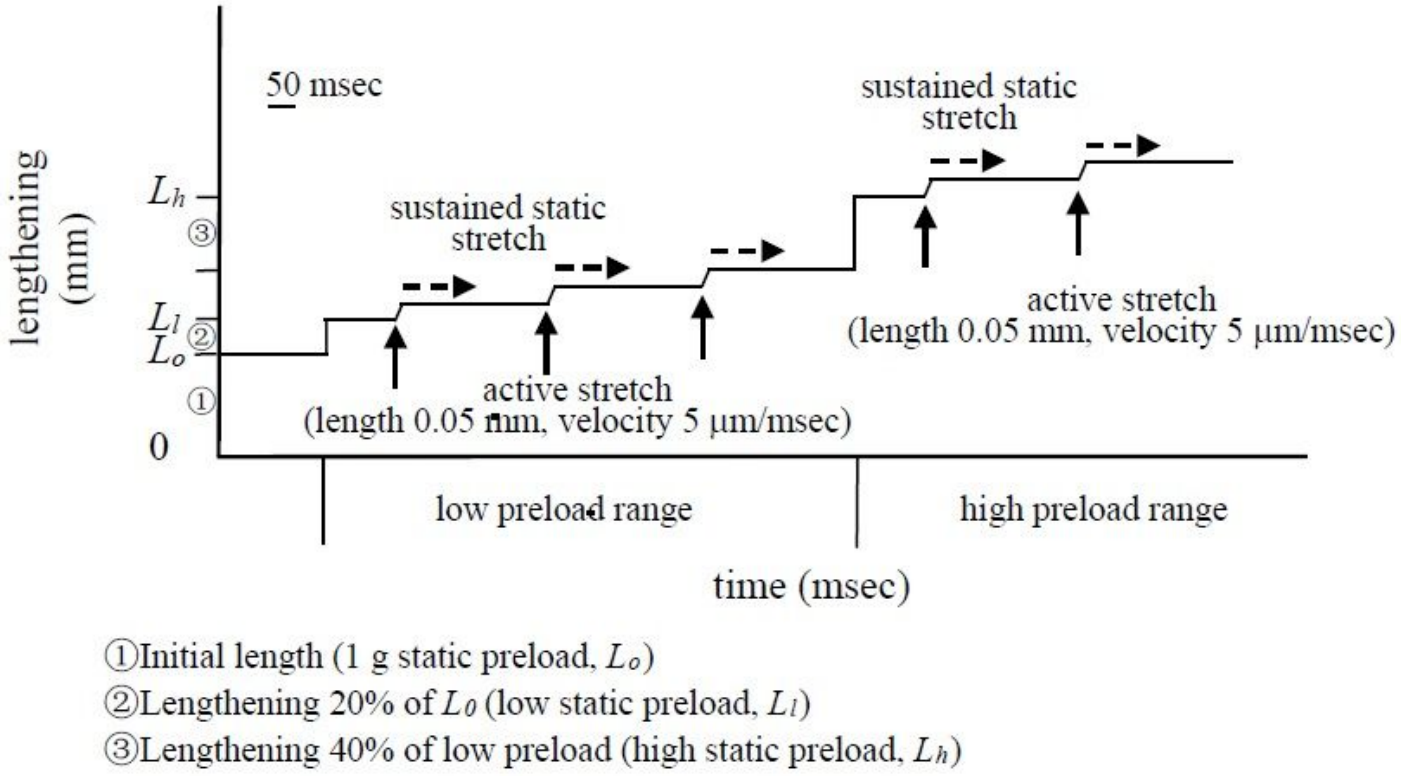


## Figure 2

The schematic diagram of lengthening stretch The sketched schematic of stretching cardiac papillary muscle fibres. The fibres were primary lengthened to obtain a 1 g initial preload (□ in y-axis, Lo). The fibres were further slowly lengthened to 20% of its initial preload (lengthening □ in y-axis), this length is defined as the low preload (Ll). The active stretch was operated under the Ll. After the low preload tests, the fibres further slowly lengthened to 40% of the ending lengthening (□ in y-axis), to obtain the high preload (Lh). The fibres were active stretch twice under the Lh. The dotted line with the arrow means fibre tolerates sustained static stretch.

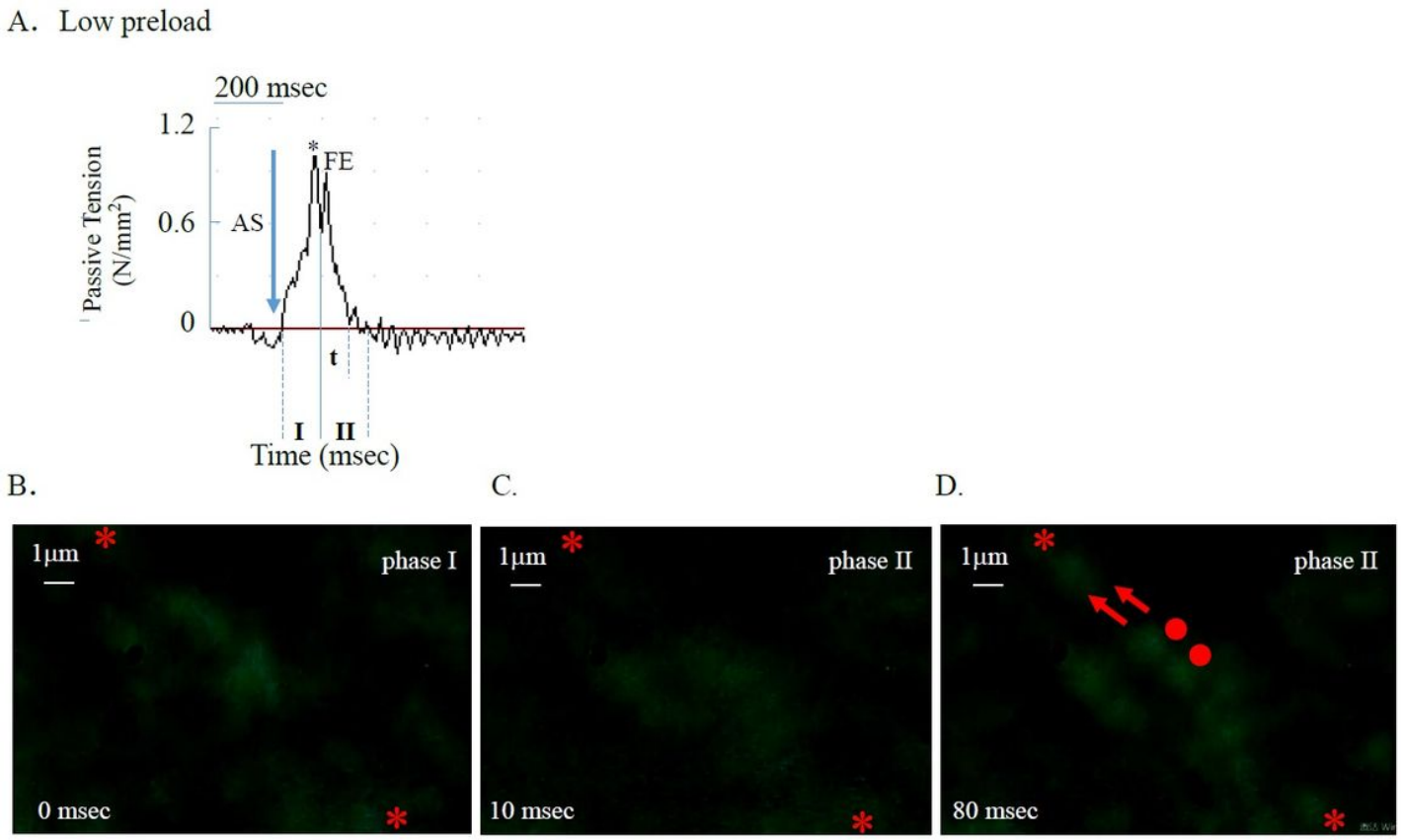


## Figure 3

Real time occurrence of spontaneous force and [Ca2+]i recruitment in stretched cardiac muscle fibre A. The myograph of one active stretch in cardiac fibre. When the fibre bearing LI, an active stretch induces a passive tension rising (AS and on time scale I; *, peak of passive tension, PTmax). Subsequently, a spontaneous isometric contraction occurred (FE, peak of force enhancement; t, force enhancement prolonging time). The fibre tolerated a sustained static stretch at this period (II, the attenuation of passive tension). EF amplitude (AIFE) normally did not surpass its PTmax. B. The fluorescence imaging of [Ca2+]i in LI cardiac fibre before active stretch. The space between * was the observing area for comparing [Ca2+]i redistribution during stretching. C. The fluorescence imaging of [Ca2+]i recruitment after one active stretch. On the myograph, the passive tension is on its attenuation phase. [Ca2+]i rapidly accumulated in the stretched fibre. D. The fluorescence imaging of [Ca2+]i transmitted after one active stretch. On the myograph, the force enhancement occurred at this time. [Ca2+]i rapidly transmitted to the adjacent fibres. The dots are the origin of Ca2+ signal, arrows are the dimension of transmitting.

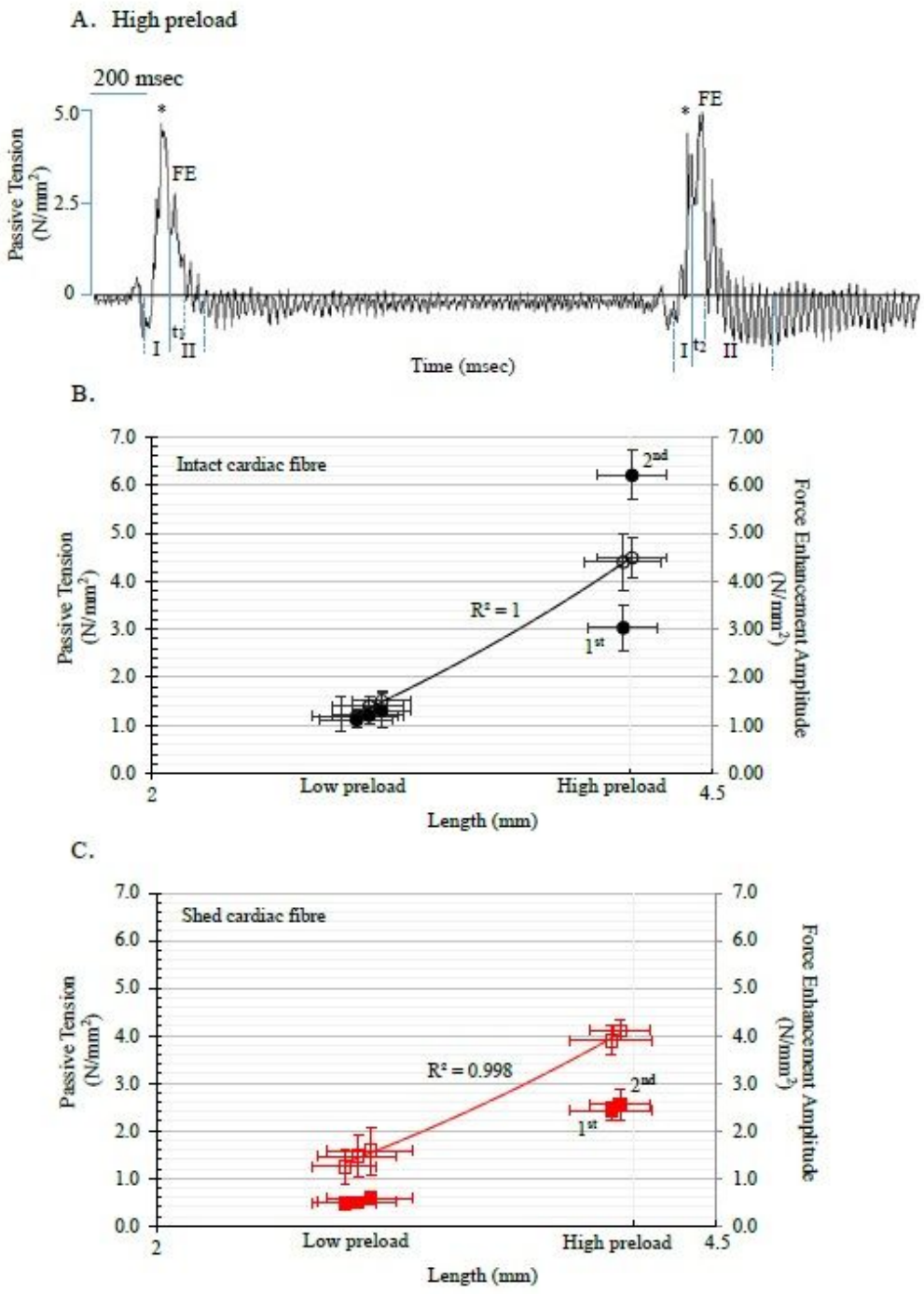


## Figure 4

Passive tension related spontaneous force enhancement in preloading cardiac fibres A. In Lh cardiac fibre, 1st and 2nd AIFE dramatically increased, furthermore the 2nd AIFE significantly surpassed its PTmax. B. PTmax presented a perfect linear correlation throughout preload range in intact cardiac fibres (R2=0.99). The AIFE significantly increased in Lh cardiac fibres. Furthermore, the 2nd AIFE surpassed its PTmax. The occurrence of spontaneous force enhancement was instability in high preload cardiac fibre. C. PTmax presented a perfect linear correlation throughout preload range in shed cardiac fibres (R2=0.99). The AIFE reduced in Lh cardiac fibres. No surpassing to its PTmax observed.

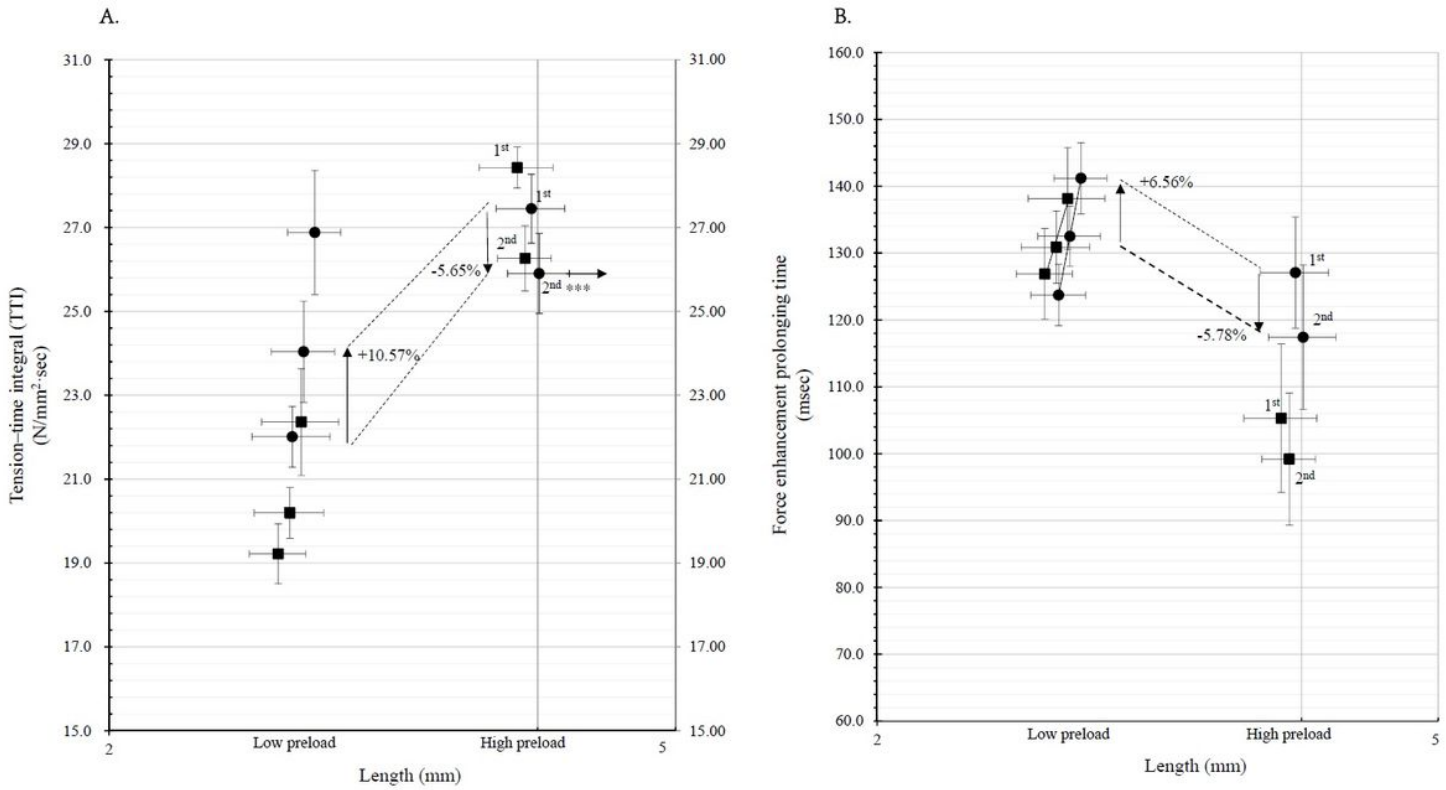


**Figure 5**

Force enhancement tension-time integral in preloading cardiac fibres A. The tension–time integral (TTI) of the force enhancement throughout the preload range of cardiac fibres. In intact fibres (black dots), TTI was significantly increased in high preload range, however, 2nd TTI significantly reduced (5.65%) because of the shortening of the prolonging time (t2). This differences presented in shed fibres as well. However, in low preload fibres the adjacent stretch induced TTI increasing (3nd 10.57% increased). B. The force enhancement prolonging time throughout the preload range of cardiac fibres. In intact fibres (black dots), t2 was significantly shortened in high preload range (5.78% shortened), however, in low preload range the last stretch induced t was extended (6.56% increased). This differences presented in shed fibres as well.

# Supplementary Files

This is a list of supplementary files associated with this preprint. Click to download.

- Thestatementofthemethodsinmanuscript.doc
- Ca2redistributioninstretchcardiacfibres.mp4